ANTHROPOLOGY

A nearly complete foot from Dikika, Ethiopia and its implications for the ontogeny and function of *Australopithecus afarensis*

Jeremy M. DeSilva[1]*, Corey M. Gill[2,3,4], Thomas C. Prang[5,6], Miriam A. Bredella[3], Zeresenay Alemseged[7]*

The functional and evolutionary implications of primitive retentions in early hominin feet have been under debate since the discovery of *Australopithecus afarensis*. Ontogeny can provide insight into adult phenotypes, but juvenile early hominin foot fossils are exceptionally rare. We analyze a nearly complete, 3.32-million-year-old juvenile foot of *A. afarensis* (DIK-1-1f). We show that juvenile *A. afarensis* individuals already had many of the bipedal features found in adult specimens. However, they also had medial cuneiform traits associated with increased hallucal mobility and a more gracile calcaneal tuber, which is unexpected on the basis of known adult morphologies. Selection for traits functionally associated with juvenile pedal grasping may provide a new perspective on their retention in the more terrestrial adult *A. afarensis*.

INTRODUCTION

Hominin foot fossils are exceptionally rare, especially those of juveniles. DIK-1-1f is a left foot found during excavation by D. Geraads on 21 January 2002 at Dikika, Ethiopia (Fig. 1 and figs. S1 and S2) about a meter away from the skull of the DIK-1-1 skeleton (*1*). It was almost entirely embedded in matrix, with only the broken surface of the tibial shaft and the broken diaphyses of the metatarsals observable externally. The partially prepared foot was briefly discussed and illustrated in the preliminary announcement (*1*). Additional preparatory work by Z.A. and C. Kiarie continued through 2013, exposing most of the elements, cemented together in an articulated foot. DIK-1-1f preserves all of the tarsals, the bases of all five metatarsals, and partial shafts of all but the first metatarsal. No pedal phalanges or metatarsal heads were recovered. There is some postdepositional shifting of the bones, although they remain in a near-anatomical position. The shafts of the metatarsals are sheared cleanly by a break that runs obliquely from the preserved epiphysis of the first metatarsal through slightly beyond the midshaft of the fifth metatarsal. There is minimal damage or surface erosion on the bones.

DIK-1-1f is the oldest hominin foot to preserve all of the tarsals. The Olduvai Hominid 8 (OH 8) foot, which is geologically much younger, is similarly complete in preserving most of the foot elements, save for the metatarsal heads and phalanges (*2*). However, there is a significant damage to the OH 8 calcaneal tuber, hindering the evaluation of important morphological information. Furthermore, DIK-1-1f preserves the elements (tarsals and proximal metatarsals) that the single adult *Australopithecus afarensis* partial forefoot (A.L. 333-115) lacks (Fig. 1) (*3*).

[1]Department of Anthropology, Dartmouth College, Hanover, NH 03755, USA. [2]Department of Anthropology, Boston University, Boston, MA 02215, USA. [3]Department of Radiology, Massachusetts General Hospital and Harvard Medical School, Boston, MA 02114, USA. [4]Department of Medicine, Icahn School of Medicine at Mount Sinai, New York, NY 10029, USA. [5]Center for the Study of Human Origins, Department of Anthropology, New York University, New York, NY 10003, USA. [6]New York Consortium in Evolutionary Anthropology, New York, NY, USA. [7]Department of Organismal Biology and Anatomy, University of Chicago, Chicago, IL 60637, USA.
*Corresponding author. Email: jeremy.m.desilva@dartmouth.edu (J.M.D.); alemseged@uchicago.edu (Z.A.)

RESULTS

DIK-1-1f measures only 54.6 mm in total proximodistal length from the calcaneal tuber to the broken metatarsal shafts. The ankle is human-like in having a moderately wedged talar trochlea with medial and lateral rims of equal height resulting in a human-like talar axis angle (fig. S3), thereby positioning the tibia orthogonally over the foot, as in *A. afarensis* adults (*4*). Humans and *A. afarensis* differ from apes in having a relatively large calcaneal tuber adaptive for dissipating loads during heel strike (*5*). Here, we find that apes have gracile calcaneal tubers as juveniles that become relatively more gracile in adults. In humans, relative calcaneal tuber cross-sectional area is high and does not change ontogenetically, indicating that humans are born with a calcaneus adapted for the rigors of heel-striking bipedalism (Fig. 2). DIK-1-1f lacks the tuber enlargement seen in young humans and is more similar to juvenile great apes. Yet, adult calcanei (A.L. 333-8, A.L. 333-37, and A.L. 333-55) are human-like in measures of relative cross-sectional area (*6*), suggesting that *A. afarensis* was characterized by an ontogenetic trajectory of calcaneal growth unique among living taxa. Similarly, while the distal calcaneus of DIK-1-1f is ape-like in being elongated and dorsoplantarly narrow, an adult *A. afarensis* has distal calcanei that are dorsoplantarly wide (fig. S4). Although *A. afarensis* adults had a robust calcaneal tuber, whether they had a human-like lateral plantar process has been questioned (*7*). The Dikika foot provides important resolution on this issue. DIK-1-1f has a human-like plantarly positioned, although weakly developed, apophyseal flange for the lateral plantar process (*5*) and lacks the beaked medial plantar process found in apes.

The evolution of obligate bipedalism resulted in the sacrifice of hallucal grasping, as evidenced by a more distally directed and mediolaterally flattened first tarsometatarsal joint in humans compared to apes (*8*). The DIK-1-1f medial cuneiform has a strongly convex distal facet for the base of the first metatarsal. In adult humans, the medial cuneiform distal facet is flat or mildly convex, but the developing osteochondral surface of the juvenile modern human medial cuneiform is convex, as found in the Dikika juvenile (fig. S5) (*9*). The curvature and angular orientation of the hallucal facet of the Dikika medial cuneiform are intermediate between gorillas and modern humans of similar size and developmental ages (Fig. 3). In humans, the ossified surface of the developing facet for the first metatarsal rapidly flattens

Fig. 1. *A. afarensis* juvenile foot DIK-1-1f. DIK-1-1f shown in (clockwise from top left) medial, dorsal, and lateral views. To right, dorsal view of DIK-1-1f and the adult *A. afarensis* foot A.L. 333-115. Scale bars, 1 cm.

with age (*9*). In contrast, apes maintain a convex surface and exhibit only moderate flattening of the ossified part of the joint surface as they grow. An adult *A. afarensis* medial cuneiform (A.L. 333-28) has a hallucal facet that is flatter than in an ape of similar size but more convex than that found in modern humans (Fig. 3) (*8*, *9*). Since A.L. 333-28 and DIK-1-1f are representatives of adult and juvenile *A. afarensis*, the change in facet curvature during growth in *A. afarensis* was probably similar to the pattern in apes and distinct from that found in humans (fig. S5). These data suggest that multidirectional loading of the hallucal tarsometatarsal joint in juveniles may have maintained the curved facet in *A. afarensis* throughout ontogeny.

The orientation of the medial cuneiform distal facet for the first metatarsal relative to the proximal navicular facet differs between humans and apes at all developmental ages (Fig. 3 and fig. S9). The Dikika juvenile has a facet angulation value intermediate between modern apes and humans. However, the adult *A. afarensis* medial cuneiform is distinctly human-like in facet orientation (*8*, *9*), indicating that the hallux may have been more medially oriented in juveniles but then became more aligned with the other rays in adult *A. afarensis*, as also occurs in *Pan* and *Homo* (*9*). Collectively, these data suggest that, while *A. afarensis* had a greater range of hallucal mobility than modern humans, they likely could not oppose the hallux with the lateral digits to the degree seen in modern apes, *Ardipithecus* (*10*), and the taxon to which the Burtele foot (BRT-VP-2/73) belongs (*11*). However, these data also suggest that juvenile *A. afarensis* may have had more hallucal mobility and abduction ability than adult *A. afarensis* and modern humans, as evidenced by its more medially oriented and convex hallucal facet.

The human cuboid contributes to midfoot rigidity and longitudinal arch support, thus differing in shape compared to great ape cuboids (*12*), but this bone was previously unknown for the genus *Australopithecus*. Unlike in modern apes, DIK-1-1f has a proximodistally elongated cuboid, especially along its lateral edge (fig. S6). The cuboid's calcaneal process is located plantarly and medially and appears more similar to the condition found in modern human juveniles. With the lateral foot in a proper anatomical position, the dorsal surface of the DIK-1-1f cuboid faces laterally, indicating the presence of a well-developed transverse arch. A transverse arch in a bipedal foot requires the external torsion of the lateral metatarsals (*13*), evident in DIK-1-1f by the orientation of the sectioned shaft of the fourth metatarsal (fig. S7). As in the human foot, the intermediate cuneiform is proximodistally elongated in DIK-1-1f (fig. S8); the adult morphology is unknown but presumed to be similarly elongated (*10*). The DIK-1-1f lateral cuneiform is somewhat foreshortened, while the adult form (A.L. 333-79) is more human-like (fig. S8). DIK-1-1f and A.L. 333-79 may be sampling a distribution of *A. afarensis* lateral cuneiform elongation greater than that found in apes but slightly less than that found in modern humans.

While it is generally accepted that *A. afarensis* had a rigid midfoot, whether it was arched or not remained controversial (*13*–*15*). The Dikika foot provides new evidence related to this key issue. The talar declination angle, thought to be related to arch height in humans (*16*, *17*), is low and ape-like in DIK-1-1f (~20°). The talocalcaneal angle is also low (~20°) and falls completely outside the range of modern humans of similar developmental age (*18*). Although the lateral aspect of the foot is rigid and a transverse arch is present, the medial portion of the foot is more plantarly positioned than in human juveniles, suggesting that a medial longitudinal arch was present but weakly developed in the Dikika individual. It is unclear whether this low arch persisted into adulthood or characterized the species or genus in general. However, a reconstruction of a composite adult foot using similarly sized tarsal remains from the A.L. 333 locality results in a foot with a similarly low talocalcaneal angle of 25° (fig. S9). While the medial midfoot of *A. afarensis* was arched compared to apes (*13*, *15*), the *A. afarensis* arch may be best characterized as low or partial relative to modern humans (*14*, *19*). Thus, critical anatomical components (that is, the long plantar ligament and a plantar aponeurosis) that are functionally important for stiffening the midfoot were likely present in *A. afarensis*, as evidenced by the presence of a scar for the long plantar ligament on the A.L. 333 calcanei, as well as its derived lateral tarsometatarsal joint morphology (*13*). Furthermore, a moderately arched foot, which may help dissipate energy during the support phase of walking and perhaps reduce the risk of lower leg

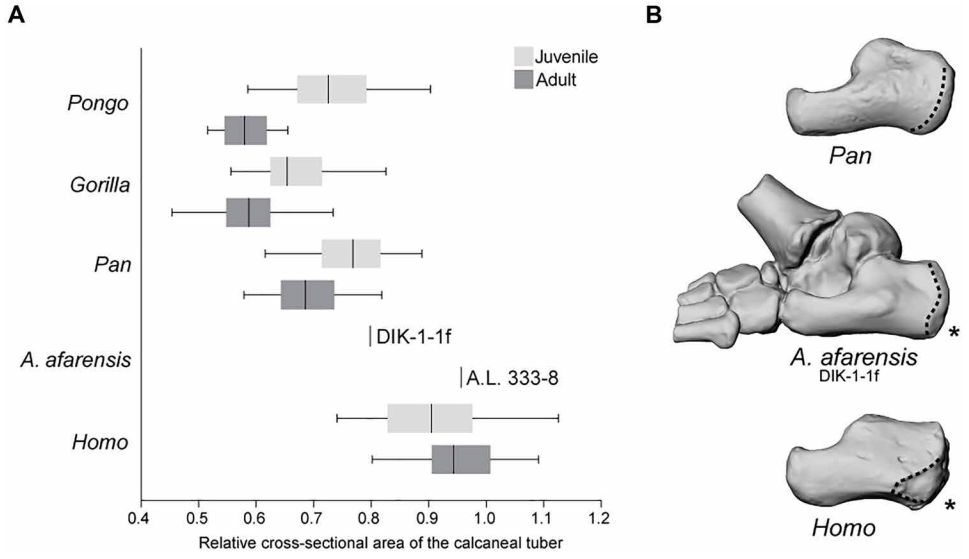

Fig. 2. Calcaneal ontogeny in apes, humans, and *A. afarensis*. (**A**) Standardized cross-sectional area of the calcaneal tuber in juvenile (light gray) and adult (dark gray) apes, *A. afarensis*, and modern humans. The vertical line represents the taxon median, the box represents the interquartile range, and the whiskers indicate the range of the data. A higher number corresponds with increased robusticity. Notice that, unlike in apes or humans, in *A. afarensis*, the calcaneus exhibits a significant developmental increase in robusticity; the Dikika juvenile is chimpanzee-like, while the Hadar adult is human-like. All juveniles are significantly different from adults for each taxon ($P \leq 0.05$) except for *Homo sapiens* ($P = 0.53$). (**B**) Three-dimensional (3D) surface renderings of DIK-1-1f, chimpanzee (top), and human (bottom) juvenile calcanei shown in lateral view. Notice the ape-like gracility of DIK-1-1f, the proximodistally long and dorsoplantarly shallow distal calcaneal region, and the large peroneal trochlea. As in humans, however, there is a plantarly positioned apophyseal flange (indicated by the asterisk) for the lateral plantar process (epiphyseal surface outlined).

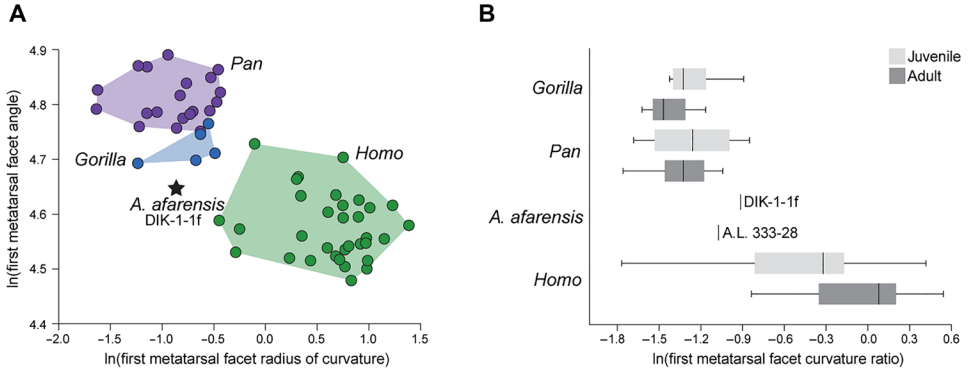

Fig. 3. Medial cuneiform ontogeny in apes, humans, and *A. afarensis*. (**A**) The radius of curvature of the distal medial cuneiform facet and the angulation of the facet relative to the navicular facet are plotted for juvenile humans (green), gorillas (blue), and chimpanzees (purple). Humans have distally directed facets (angle ~90° to 100°), with facet convexity that ranges from ape-like in small juveniles (see fig. S5) to flatter joints in subadults (*9*). Ape juveniles have convex, medially directed facets. The DIK-1-1f morphology is intermediate between humans and gorillas, with a facet orientation between human and ape, and a more ape-like joint convexity. (**B**) When standardized by the dorsoplantar height of the medial cuneiform, facet curvature can be assessed independent of size. While facet curvature differs little between juvenile and adult apes, humans experience a developmental flattening of the joint with growth. Both DIK-1-1f and A.L. 333-28 are more convex than similarly sized humans but less so than apes and, when paired, have the ape-like pattern of maintained convexity with growth of the bone (fig. S5). The box-and-whiskers plot shows the mean (dark vertical line), upper and lower quartiles (boxes), and range (whiskers).

injury (*20*), appears to be present in *A. afarensis* (*13*, *15*). However, a fully arched foot, which is hypothesized to stretch, recoil, and generate elastic energy during running (*21*, *22*), may not have typified *A. afarensis* (*14*, *19*).

DISCUSSION

The Dikika foot preserves elements previously unknown for *Australopithecus* and allows for the study of ontogeny in an extinct hominin foot for the first time. Studies of ontogeny offer an alternative perspective on the evolution of adult phenotypes since selection may act directly on juveniles and patterns of development. However, the ontogeny of the hominin foot has been poorly understood, primarily owing to a lack of fossil evidence. As previously documented, the *A. afarensis* foot was well-adapted for habitual bipedalism (*4*–*6*, *13*, *19*, *23*). This species had a talocrural joint orthogonal to the long axis of the tibia, aligning the ankle and knee under the body's center of mass. While *A. afarensis* had a large

Table 1. DIK-1-1f comparative anatomy. ML, mediolaterally; DP, dorsoplantarly; PD, proximodistally.

Bone	Human-like features	Ape-like features	Adult *A. afarensis* features	Developmental changes in *A. afarensis* morphology
Calcaneus	Lateral plantar process apophyseal flange position	Secondary ossification center for peroneal tubercle	Large depression for calcaneofibular ligament	Gracile in juvenile; becomes more robust in adults
	Plantarly wide (ML) tuber	DP short and vertical cuboid facet	Small lateral plantar process apophyseal surface	Rugosity for lateral plantar ligament not present in DIK; present in adults
	Medial tubercle flat (not beaked)	Medially angled distal calcaneus at peroneal trochlea inflection point		Low DP height of distal calcaneus; enlarges in adults
Talus	Moderately wedged	ML broad talar head	Weak angle of declination	Head expands DP
	Equal heights of trochlear rims			
	ML flat trochlear body			
	Talar axis angle			
Cuboid	PD elongated laterally	Articulates with navicular	Unknown	Unknown
	Dorsal surface twisted to face laterally			
	Beak eccentrically positioned			
Medial cuneiform	Distally positioned tibialis anterior sub-bursal sulcus	ML convex Mt1 surface	ML convexity and angulation of Mt1 surface greater than in humans; less than in apes	Mt1 facet maintains convexity developmentally
				Mt1 facet becomes less medially oriented
Lateral cuneiform	Contact facet with Mt4	PD foreshortened	Transverse arch more developed than in apes; less developed than in humans (especially medially)	Juvenile is PD short and becomes more elongated with age
Intermediate cuneiform	Nested into angled lateral surface of medial cuneiform			Unknown
Navicular		Facet for medial cuneiform slightly convex DP and ML		
Metatarsals	Strong external torsion Mt4 Mt4 base DP tall	Mt2 proximal base weakly angled ML		Mt2 base enlarges DP

calcaneal tuber important for dissipating the forces of impact during heel-striking bipedalism (*5*, *6*), the development of this robusticity was delayed compared to modern humans. The lateral metatarsal bases were relatively tall (fig. S10), and the cuboid was elongated, helping produce a stiff midfoot that increases leverage during the propulsive phase of walking, although recent works have challenged the dichotomization of the human midfoot as rigid and the ape foot as mobile (*24*, *25*).

The more ape-like features in the juvenile calcaneus and medial cuneiform, combined with their unique pattern of ontogeny, demonstrate that there is no living analog for the *A. afarensis* foot (Table 1). The longitudinal arch was weakly developed, with the medial aspect of the foot positioned more plantarly than in modern humans. The hallux could not be abducted to the degree seen in apes and *Ardipithecus* (*10*), but there is retained convexity of the medial cuneiform facet for the first metatarsal from infancy into adulthood, suggesting less stereotyped loading of the hallucal tarsometatarsal joint compared to modern humans, which may be associated with increased range of mobility at this joint in *A. afarensis* (*26*). These anatomies would produce a less effective windlass mechanism (*27*) and, thus, a push-off phase of bipedal gait that differed slightly from that found in humans today (*28*). Furthermore, increased mobility at the hallucal tarsometatarsal joint may have been advantageous during the exploitation of arboreal resources for sustenance or safety (*29*–*32*). The Dikika child was similar in size to a chimpanzee of comparable age and was likely still dependent on and perhaps often actively carried by adults. Given the energetic costs of infant carrying (*33*), both adults and juveniles may have benefitted from the hallucal mobility present in the juvenile foot of *A. afarensis*.

The DIK-1-1 skeleton offers a novel perspective on the paleobiology of a long-studied and often controversial species by preserving features that track locomotor adaptation (*1*, *29*, *34*). Owing to its developmental stage, DIK-1-1f contributes a unique window into the ontogenetic development of bipedal adaptations in the foot of *A. afarensis*. At 3.32 million years old, DIK-1-1f provides evidence for habitual bipedality combined with some pedal grasping in the juvenile australopith. Evolutionary theory predicts that selection should act strongly on juveniles. Selection for traits associated with juvenile pedal grasping in the context of arboreality or infant dependency may offer a new perspective for the retention of ape-like traits in the occasionally arboreal but otherwise more terrestrial, adult *A. afarensis*.

MATERIALS AND METHODS

Preservation

DIK-1-1f preserves all seven tarsals and the bases of the five metatarsals. The bones were recovered in a near-anatomical position; however, the bones did shift slightly. The distal tibia is hyperdorsiflexed on the talus. The tibial metaphysis has slid laterally relative to the epiphysis, and the shaft is tilted in a valgus orientation. This is unlikely to have been the position in life, given the human-like talar axis angle (fig. S3) and an isolated right distal tibia from DIK-1-1 that has an orthogonal talar surface relative to the shaft. The talus has slight distal shifting off the calcaneus and is highly plantarflexed, while the calcaneus has slightly shifted into an inverted position. The transverse tarsal region, consisting of the navicular, intermediate, and lateral cuneiforms, is shifted dorsally. This is particularly true for the navicular. This dorsal shifting may have been a result of mediolateral compression of the foot. Most of this compression has occurred medially, shifting the medial cuneiform and medial metatarsal shafts laterally and plantarly. The fifth metatarsal has externally rotated so that the facet for the fourth metatarsal is facing plantarly. In addition, it has shifted laterally so that it is no longer in articulation with the cuboid. The second metatarsal has been slightly displaced distally. The epiphysis of the first metatarsal has rotated externally so that the medial aspect is facing plantarly. Note that, while there has been shifting of bones relative to one another, there is no evidence for any distortion of the individual bones. While the bones remain conjoined, the shifting of the elements described above has resulted in enough separation between individual elements to take the measurements described in this paper. Some anatomies (for example, the subtalar joint) remain obscured. Digital preparation of the individual elements is underway.

Developmental approach

Developmentally, both in terms of size and ossification of the tarsals, DIK-1-1f best matches chimpanzees that had fully erupted, occluded, but unworn M_1. Human skeletal material that developmentally resembled DIK-1-1f had M_1's in the process of erupting. Using the skeletal maturity indicators, DIK-1-1f is developmentally similar to a human foot between 4.5 and 6 years of age (*35*). The cuboid has a clear peroneal groove [plate 17 in (*35*)], whereas the navicular has not yet formed fully reciprocal joints with the cuneiforms [plate 18 in (*35*)]. Preliminary estimates of ~3 years for the chronological age of the Dikika child (*1*) would indicate that *A. afarensis* feet matured more rapidly than human feet today.

In part because of the difficulty in finding a complete set of tarsals from skeletonized ape or human juvenile remains, our sample sizes differ from element to element, and each is described in turn below. Extant ape and human specimens were measured at the American Museum of Natural History (AMNH), the Cleveland Museum of Natural History (CMNH), the Academy of Natural Sciences Philadelphia (ANSP), the U.S. National Museum (USNM), the Harvard Museum of Comparative Zoology (MCZ), the Harvard Peabody Museum of Archaeology and Ethnology, the Libben collection at Kent State University, the Center for the Study of Human Origins at New York University (CSHO), and Stony Brook University (SBU).

We assessed each element using ontogenetic sequence allometry methods in which the trait of choice was measured against some measure of size. These measurements were first $\log_{10}$-transformed. In addition, simple ratios between the trait in question and the measure of size were used to characterize DIK-1-1f compared with juvenile and adult extant apes and modern humans. Juveniles were defined on the basis of the presence of unfused growth plates in the long bones and unerupted dentition.

Calcaneal robusticity

The modern human sample is mostly composed of individuals of European, African-American, and Asian descent but also includes three individuals from the Andaman Islands and one small-bodied Mbuti individual. A NextEngine desktop laser scanner was used to create 3D models of each bone. Most specimens in this study were scanned in at least two orientations with 10 rotations per orientation at a resolution of 10,000 points per 645.2 mm^2. Each orientation produced a triangular mesh that was imported into Geomagic Studio software for filling holes, cleaning imperfections, and merging with meshes of subsequent orientations to produce a complete 3D model.

A measure of relative calcaneal tuber robusticity was quantified as calcaneal tuber cross-sectional area per square geometric mean following the methods in (*6*). The calcaneus geometric mean included the following six metrics: (i) proximodistal tuber length, (ii) proximodistal neck length, (iii) minimum dorsoplantar tuber height, (iv) dorsoplantar neck height, (v) minimum mediolateral tuber width, and (vi) mediolateral tuber width at the peroneal trochlea. Calcaneal tuber length was measured by orienting each model in dorsal view and measuring the linear distance between the center of the posterior talar facet and the most dorsal aspect of the posterior tuber. Calcaneal neck length was defined as the linear distance between the center of the posterior talar facet to the most dorsal point on the distal margin of the cuboid facet. The dorsoplantar height of the neck was measured as the linear distance between a point distal to the posterior talar facet dorsally to the most plantar aspect of the neck, which most often included the area of bony buildup associated with the short plantar ligament. The mediolateral width of the tuber at the peroneal trochlea was measured as the linear distance between the most lateral point on the peroneal trochlea to the most medial point on the tuber, which was often adjacent to the lateral margin of the flexor hallucis longus groove beneath the sustentaculum tali. These measurements were taken on calcanei from adult *H. sapiens* ($n = 37$), *Pan troglodytes* ($n = 25$), *Gorilla gorilla* ($n = 25$), and *Pongo pygmaeus* ($n = 14$) and from juvenile *H. sapiens* ($n = 28$), *P. troglodytes* ($n = 32$), *G. gorilla* ($n = 18$), and *P. pygmaeus* ($n = 13$).

Univariate pairwise comparisons were conducted to assess the quantitative differences between extant taxa. When multiple comparisons are conducted, the chance of obtaining a type I error, or the incorrect rejection of a true null hypothesis, is increased. The standard α value of 0.05 was modified using Tukey's pairwise comparisons. All statistical analyses were conducted using PAST (PAleontological STatistics) (*36*, *37*).

Calcaneal growth

As described above, two linear measurements were taken on mixed-age calcanei from *H. sapiens* ($n = 42$), *P. troglodytes* ($n = 60$), *Pan paniscus* ($n = 6$), *G. gorilla gorilla* ($n = 17$), and *P. pygmaeus* ($n = 9$): maximum calcaneal length and distal calcaneal height. Distal calcaneal height was measured as the minimum dorsoplantar height perpendicular to the distal edge of the proximal talar facet. Total calcaneal length in A.L. 333-8 was estimated by regressing total calcaneal length against maximum preserved length in A.L. 333-8 in humans ($n = 5$), chimpanzees ($n = 4$), gorillas ($n = 4$), and the fossil calcaneus Omo-33-74-896. Maximum calcaneal length was measured as the linear

distance between the most dorsal point on the calcaneocuboid joint to the most proximal point on the triceps surae insertion. Minimum calcaneal length was measured as the distance between the most proximal point on the triceps surae insertion to the most distal point on the short plantar ligament insertion beneath the plantar margin of the calcaneocuboid joint.

Talus

Talar axis angle and wedging were assessed using the methods described elsewhere (*38*). In short, two measurements were taken: the mediolaterally widest aspect of the anterior (or distal) talar trochlea from the rim of the cotylar fossa to the distolateral edge of the trochlea and the mediolaterally widest aspect of the posterior (or proximal) talar trochlea. These measurements were taken from mixed-aged tali from *H. sapiens* ($n = 101$), *G. gorilla gorilla* ($n = 55$), *P. troglodytes* ($n = 71$), *P. paniscus* ($n = 6$), and *P. pygmaeus* ($n = 56$). The talar axis angle was calculated as described elsewhere (*38*). In short, the talus was digitally isolated using DeskArtes, and a horizontal line was drawn through the dorsal surface of the talar trochlea. Another line was drawn through the inferior edges of the cotylar fossa and the fibular facet. The angle between these lines was measured using ImageJ and compared with an adult sample of humans ($n = 45$), chimpanzees ($n = 51$), and gorillas ($n = 45$), as previously published (*38*). The talar axis angle was taken on juveniles *H. sapiens* ($n = 27$), *G. gorilla gorilla* ($n = 9$), and *P. troglodytes* ($n = 20$) using the methods described above using images of the talus taken in posterior view. Because the DIK-1-1f talus is still articulated with the other foot elements, this measurement should be considered an estimate and revisited when the talus has been digitally isolated.

Navicular

The navicular is the last tarsal to fully ossify (*35*) and yields the least amount of information in the DIK-1-1f. The navicular tuberosity, which forms from a secondary ossification center, either had not begun to ossify or was not preserved in DIK-1-1f. Facets for the cuneiforms lacked defined edges delineating articular facets from nonarticular regions of the bone.

Medial cuneiform

This bone was examined in adult *H. sapiens* ($n = 20$), *G. gorilla gorilla* ($n = 36$), and *P. troglodytes* ($n = 36$) and in juveniles of *H. sapiens* ($n = 37$), *G. gorilla gorilla* ($n = 6$), and *P. troglodytes* ($n = 24$). A.L. 333-28 was studied at the National Museum of Ethiopia (Addis Ababa). Human samples were obtained through a retrospective search of nonpathological computed tomography (CT) scans of the foot at Massachusetts General Hospital ($n = 47$). That aspect of the study was approved by the Partners Healthcare Inc. Institutional Review Board and complied with the Health Insurance Portability and Accountability Act. Ten skeletonized adult medial cuneiforms from the Boston University Biological Anthropology Laboratory were also included. In vivo CT imaging was performed using a GE LightSpeed Pro 16 scanner (General Electric): slice thickness, 2.5 mm; tube voltage, 120 kV; average tube current-time, 300 mA·s. Dry bone and casts of hominin fossils were scanned using a Planmed Verity (Planmed Oy) CT scanner: slice thickness, 400 μm; tube voltage, 90 kV; average tuber current-time, 3.8 mA·s. Because CT was used, soft tissue and cartilage were not captured in the resulting 3D surface renderings that were used to quantify facet orientation or curvature. Yet, note that we were limited to quantifying only the osseous portion of the medial cuneiform in juveniles and are well aware that endochondral ossification was still occurring in these individuals. Thus, the shape of the preserved osteochondral interface quantified may not precisely mirror the shape of the joint surface. Nevertheless, through chondral modeling (*39*), the articular cartilage layer eventually becomes congruent with the underlying subchondral bone, and in this study and elsewhere (*9*), we characterized the developmental trajectory by which this adult shape was achieved. Nevertheless, note that the DIK-1-1f medial cuneiform has well-defined edges delineating the smooth articular Mt1 facet from the nonarticular regions of the bone. It is comparable to human medial cuneiforms between 4.5 and 6 years of age (*35*), and it is known that the adult morphology of the medial cuneiform has been achieved by the age of 6 years in humans (*40*) although adult size has not. Measurements on these scanned medial cuneiforms were taken in a Picture Archiving and Communication System viewer (OsiriX software version 5.8.5, Pixmeo SARL) and described in more detail elsewhere (*9*). Briefly, the radius of curvature of the first metatarsal facet was measured on the transverse slice of axial images corresponding to the middle of the navicular facet using the ROI tool. A circle was fitted to maximize contact with the facet. How radius of curvature changed during growth in humans and apes was assessed as a function of the maximum dorsoplantar height of the medial cuneiform. Because of damage to the bone dorsally, only 22.5 mm of the dorsoplantar height was preserved. The full dorsoplantar height of A.L. 333-28 was estimated to be 29.5 mm by taking the ratio of the maximum proximodistal length to the dorsoplantar height in the StW 573 and OH 8 medial cuneiforms and applying it to A.L. 333-28. Medial angulation of the first metatarsal facet was quantified as described elsewhere (*8*, *9*). In short, points were placed along the lateral edge of the navicular facet, as well as on the medial and lateral edges of the distal facet. An angulation tool was used to connect these to yield medial angulation in degrees.

Lateral and intermediate cuneiforms

Two measurements were taken on both the lateral and intermediate cuneiforms: the maximum mediolateral width of the bone and the maximum proximodistal length. These measures were taken on the lateral cuneiform of juvenile and adult *H. sapiens* ($n = 43$), *G. gorilla gorilla* ($n = 40$), *P. troglodytes* ($n = 80$), *P. paniscus* ($n = 5$), and *P. pygmaeus* ($n = 8$). These measures were taken on the intermediate cuneiform of juvenile and adult *H. sapiens* ($n = 43$), *G. gorilla gorilla* ($n = 39$), *P. troglodytes* ($n = 74$), *P. paniscus* ($n = 5$), and *P. pygmaeus* ($n = 8$). A.L. 333-79 was measured at the National Museum of Ethiopia in Addis Ababa.

Cuboid

Three measurements were taken on juvenile and adult cuboids from *H. sapiens* ($n = 32$), *G. gorilla gorilla* ($n = 19$), *P. troglodytes* ($n = 59$), *P. paniscus* ($n = 6$), and *P. pygmaeus* ($n = 9$): the maximum mediolateral width of the cuboid, the maximum medial proximodistal length from the edge of the facet with the fourth metatarsal to the edge of the facet with the calcaneus, and the maximum lateral proximodistal length from the edge of the facet with the fifth metatarsal to the edge of the facet with the calcaneus.

Metatarsals

Measurements were taken primarily on the second and fourth metatarsals. These included the maximum length, maximum mediolateral width of the metatarsal base, and the maximum dorsoplantar height of the metatarsal base. Comparative measurements were taken on mixed-aged second metatarsals from *H. sapiens* ($n = 34$), *G. gorilla gorilla* ($n = 17$),

P. troglodytes ($n = 50$), *P. paniscus* ($n = 5$), and *P. pygmaeus* ($n = 9$) and on mixed-aged fourth metatarsals from *H. sapiens* ($n = 39$), *G. gorilla gorilla* ($n = 16$), *P. troglodytes* ($n = 53$), *P. paniscus* ($n = 5$), and *P. pygmaeus* ($n = 9$). In addition, fourth metatarsal torsion was measured on juvenile *H. sapiens* ($n = 14$) and *P. troglodytes* ($n = 10$) and compared with published data on torsion in adult specimens (*13*). Torsion was measured by aligning the dorsum of the metatarsal base along a horizontal plane and photographing the distal metatarsal (either the head if the epiphysis was attached or the epiphyseal surface). The photograph was imported into ImageJ, and the angle between the long axis of the head (or epiphyseal surface) and the horizontal plane of the dorsal surface of the base was measured. These measurements were compared with and fall within the range of distribution found in adult fourth metatarsals of the same species (*13*). Metatarsal torsion was measured the same way in DIK-1-1f, but the bone was broken along the distal shaft and, thus, was only roughly comparable to the extant sample. Data from A.L. 333-160 and BRT-VP-2/73 (Burtele) were obtained from published measurements (*11*, *13*). A.L. 333-133 was measured at the Ethiopia National Museum in Addis Ababa.

Longitudinal arch

A composite adult *A. afarensis* foot was assembled from four right tarsals from the 333 locality: A.L. 333-8 (calcaneus), A.L. 333-147 (talus), A.L. 333-36 (navicular), and A.L. 333-28 (medial cuneiform). Original fossils were studied in the Ethiopia National Museum in Addis Ababa. Casts of all specimens were used to assemble the composite foot. Observations on the original fossils strongly suggest that A.L. 333-36 and A.L. 333-28 belong to the same individual based on joint congruence and shared patina. It is unclear whether the other fossils belong to the same individual, although on the basis of joint congruence, it is unlikely that A.L. 333-147 and A.L. 333-8 are from the same individual. Therefore, we acknowledge that we are only crudely measuring the morphology of the *A. afarensis* foot using the methods presented here. The casts were manually assembled using museum putty and by maximizing congruence between the joint surfaces through visual inspection. When fully assembled, the composite foot was photographed in medial view. The talocalcaneal angle was measured using ImageJ. A line was drawn along the plantar surface of the calcaneus and extended distally. A second line was drawn to bisect the talar neck and head and the medial cuneiform. The angle between the two lines is the talocalcaneal angle. The Hadar composite was reconfigured on five separate occasions, and this measurement was retaken. Each time, the measurement was ~25°. The same bones were assembled on seven different *P. troglodytes* and *G. gorilla* feet and measured in the same manner, yielding talocalcaneal angles of 16.6° (range, 13.6° to 20.1°). The angle was measured on DIK-1-1f in the same manner. However, note that there has been some post mortem shifting of the foot bones of DIK-1-1f such that the talus has slid slightly laterally and proximally off the sustentaculum tali and the navicular has moved dorsally. In addition, there is some evidence for mediolateral forces that compressed the foot, given that the epiphysis for Mt1 and the Mt5 shaft have both rotated. Even given these modifications to the DIK-1-1f, we measured a talocalcaneal angle near to that found in the adult *A. afarensis* foot. Talar declination angle was measured following (*16*).

SUPPLEMENTARY MATERIALS

Supplementary material for this article is available at http://advances.sciencemag.org/cgi/content/full/4/7/eaar7723/DC1

Supplementary Text

Fig. S1. The discovery of DIK-1-1f by D. Geraads on 21 January 2002 during excavation at DIK-1 locality.
Fig. S2. DIK-1-1f in various views.
Fig. S3. Talus ontogeny in apes, humans, and *A. afarensis*.
Fig. S4. Calcaneal ontogeny in apes, humans, and *A. afarensis*.
Fig. S5. Medial cuneiform ontogeny in apes, humans, and *A. afarensis*.
Fig. S6. Cuboid ontogeny in apes, humans, and *A. afarensis*.
Fig. S7. A clean section through the metatarsal shafts of the articulated DIK-1-1f shows the transverse arch of this foot.
Fig. S8. Compared to the apes, humans have proximodistally elongated cuneiforms.
Fig. S9. The calcaneus, talus, navicular, and medial cuneiform have been rearticulated in a human, chimpanzee, gorilla, DIK-1-1f, and a composite Hadar foot.
Fig. S10. Metatarsal base ontogeny in apes, humans, and *A. afarensis*.
Data file S1. Raw measurements used in this study.

REFERENCES AND NOTES

1. Z. Alemseged, F. Spoor, W. H. Kimbel, R. Bobe, D. Geraads, D. Reed, J. G. Wynn, A juvenile early hominin skeleton from Dikika, Ethiopia. *Nature* **443**, 296–301 (2006).
2. M. H. Day, J. R. Napier, Hominid fossils from Bed I, Olduvai Gorge, Tanganyika: Fossil foot bones. *Nature* **201**, 969–970 (1964).
3. B. M. Latimer, C. O. Lovejoy, D. C. Johanson, Y. Coppens, Hominid tarsal, metatarsal, and phalangeal bones recovered from the Hadar Formation: 1974–1977 collections. *Am. J. Phys. Anthropol.* **57**, 701–719 (1982).
4. B. M. Latimer, J. C. Ohman, C. O. Lovejoy, Talocrural joint in African hominoids: Implications for *Australopithecus afarensis*. *Am. J. Phys. Anthropol.* **74**, 155–175 (1987).
5. B. Latimer, C. O. Lovejoy, The calcaneus of *Australopithecus afarensis* and its implications for the evolution of bipedality. *Am. J. Phys. Anthropol.* **78**, 369–386 (1989).
6. T. C. Prang, Calcaneal robusticity in Plio-Pleistocene hominins: Implications for locomotor diversity and phylogeny. *J. Hum. Evol.* **80**, 135–146 (2015).
7. R. L. Susman, J. T. Stern Jr., W. L. Jungers, Arboreality and bipedality in the Hadar hominids. *Folia Primatol.* **43**, 113–156 (1984).
8. B. Latimer, C. O. Lovejoy, Hallucal tarsometatarsal joint in *Australopithecus afarensis*. *Am. J. Phys. Anthropol.* **82**, 125–133 (1990).
9. C. M. Gill, M. A. Bredella, J. M. DeSilva, Skeletal development of hallucal tarsometatarsal joint curvature and angulation in extant apes and modern humans. *J. Hum. Evol.* **88**, 137–145 (2015).
10. C. O. Lovejoy, B. Latimer, G. Suwa, B. Asfaw, T. D. White, Combining prehension and propulsion: The foot of *Ardipithecus ramidus*. *Science* **326**, 72–72e8 (2009).
11. Y. Haile-Selassie, B. Z. Saylor, A. Deino, N. E. Levin, M. Alene, B. M. Latimer, A new hominin foot from Ethiopia shows multiple Pliocene bipedal adaptations. *Nature* **483**, 565–569 (2012).
12. F. Bojsen-Møller, Calcaneocuboid joint and stability of the longitudinal arch of the foot at high and low gear push off. *J. Anat.* **129**, 165–176 (1979).
13. C. V. Ward, W. H. Kimbel, W. C. Johanson, Complete fourth metatarsal and arches in the foot of *Australopithecus afarensis*. *Science* **331**, 750–753 (2011).
14. W. E. H. Harcourt-Smith, L. C. Aiello, Fossils, feet and the evolution of human bipedal locomotion. *J. Anat.* **204**, 403–416 (2004).
15. T. C. Prang, Rearfoot posture of *Australopithecus sediba* and the evolution of the hominin longitudinal arch. *Sci. Rep.* **5**, 17677 (2015).
16. M. H. Day, B. A. Wood, Functional affinities of the Olduvai Hominid 8 talus. *Man* **3**, 440–455 (1968).
17. K. Peeters, J. Schreuer, F. Burg, C. Behets, S. Van Bouwel, G. Dereymaeker, J. V. Sloten, I. Jonkers, Altered talar and navicular bone morphology is associated with pes planus deformity: A CT-scan study. *J. Orthop. Res.* **31**, 282–287 (2013).
18. R. Vanderwilde, L. T. Staheli, D. E. Chew, V. Malagon, Measurements on radiographs of the foot in normal infants and children. *J. Bone Joint Surg.* **70**, 407–415 (1988).
19. T. C. Prang, Reevaluating the functional implications of *Australopithecus afarensis* navicular morphology. *J. Hum. Evol.* **97**, 73–85 (2016).
20. A. Simkin, I. Leichter, M. Giladi, M. Stein, C. Milgrom, Combined effect of foot arch structure and an orthotic device on stress fractures. *Foot Ankle Int.* **10**, 25–29 (1989).
21. R. F. Ker, M. B. Bennett, S. R. Bibby, R. C. Kester, R. McN. Alexander, The spring in the arch of the human foot. *Nature* **325**, 147–149 (1987).
22. D. P. Perl, A. I. Daoud, D. E. Lieberman, Effects of footwear and strike type on running economy. *Med. Sci. Sports Exerc.* **44**, 1335–1343 (2012).
23. C. V. Ward, Interpreting the posture and locomotion of *Australopithecus afarensis*: Where do we stand? *Am. J. Phys. Anthropol.* **119**, 185–215 (2002).
24. K. T. Bates, D. Collins, R. Savage, J. McClymont, E. Webster, T. C. Pataky, K. D'Aout, W. I. Sellers, M. R. Bennett, R. H. Crompton, The evolution of compliance in the human lateral mid-foot. *Proc. Biol. Sci.* **280**, 20131818 (2013).

25. N. B. Holowka, M. C. O'Neill, N. E. Thompson, B. Demes, Chimpanzee and human midfoot motion during bipedal walking and the evolution of the longitudinal arch of the foot. *J. Hum. Evol.* **104**, 23–31 (2017).
26. D. J. Proctor, Brief communication: Shape analysis of the MT 1 proximal articular surface in fossil hominins and shod and unshod *Homo*. *Am. J. Phys. Anthropol.* **143**, 631–637 (2010).
27. N. L. Griffin, C. E. Miller, D. Schmitt, K. D'Août, Understanding the evolution of the windlass mechanism of the human foot from comparative anatomy: Insights, obstacles, and future directions. *Am. J. Phys. Anthropol.* **156**, 1–10 (2015).
28. P. J. Fernández, N. B. Holowka, B. Demes, W. L. Jungers, Form and function of the human and chimpanzee forefoot: Implications for early hominin bipedalism. *Sci. Rep.* **6**, 30532 (2016).
29. D. J. Green, Z. Alemseged, *Australopithecus afarensis* scapular ontogeny, function, and the role of climbing in human evolution. *Science* **338**, 514–517 (2012).
30. J. T. Stern Jr., R. L. Susman, The locomotor anatomy of *Australopithecus afarensis*. *Am. J. Phys. Anthropol.* **60**, 279–317 (1983).
31. V. V. Venkataraman, T. S. Kraft, N. J. Dominy, Tree climbing and human evolution. *Proc. Natl. Acad. Sci. U.S.A.* **110**, 1237–1242 (2013).
32. C. B. Ruff, M. L. Burgess, R. A. Ketcham, J. Kappelman, Limb bone structural properties and locomotor behavior in A.L. 288-1 ("Lucy"). *PLOS ONE* **11**, e0166095 (2016).
33. C. M. Wall-Scheffler, K. Geiger, K. L. Steudel-Numbers, Infant carrying: The role of increased locomotory costs in early tool development. *Am. J. Phys. Anthropol.* **133**, 841–846 (2007).
34. C. V. Ward, T. K. Nalley, F. Spoor, P. Tafforeau, Z. Alemseged, Thoracic vertebral count and thoracolumbar transition in *Australopithecus afarensis*. *Proc. Natl. Acad. Sci. U.S.A.* **114**, 6000–6004 (2017).
35. N. L. Hoerr, S. L. Pyle, C. C. Francis, *Radiographic Atlas of Skeletal Development of the Foot and Ankle: A Standard of Reference* (Thomas Publishers, 1962).
36. Ø. Hammer, D. A. T. Harper, P. D. Ryan, PAST-Palaeontological statistics (2001); https://folk.uio.no/ohammer/past/.
37. Ø. Hammer, D.A.T. Harper, PAST version 1.57. Norway: Natural History Museum, University of Oslo (2006).
38. J. M. DeSilva, Functional morphology of the ankle and the likelihood of climbing in early hominins. *Proc. Natl. Acad. Sci. U.S.A.* **106**, 6567–6572 (2009).
39. M. W. Hamrick, A chondral modeling theory revisited. *J. Theor. Biol.* **201**, 201–208 (1999).
40. L. Scheuer, S. Black, *Developmental Juvenile Osteology* (Elsevier, 2000).

Acknowledgments: We thank the Authority for Research and Conservation of Cultural Heritage and its personnel for making the field and laboratory work possible. We are grateful to E. Westwig (AMNH); Y. Haile-Selassie and L. Jellema (CMNH); O. Lovejoy (Libben; Kent State University); J. Chupasko (MCZ); D. Pilbeam, M. Morgan, and O. Herschensohn (Harvard Peabody); N. Gilmore (ANSP); D. Lunde (USNM); H. Taboada (CSHO); and W. Jungers (SBU) for the access to skeletal material in their care. We thank W. Kimbel for permission to study Hadar fossils. We thank F. Spoor and B. Latimer for providing helpful comments on an earlier version of this manuscript and feedback from the participants of the Dikika Workshops. We are grateful to W. Jungers, W. Harcourt-Smith, an anonymous reviewer, and the editors of *Science Advances* for providing constructive feedback. **Funding:** Comparative and fossil preparation work and pertinent workshops were supported by Margaret and Will Hearst. Members of the Dikika Research Project contributed toward the discovery of the fossil reported here. **Author contributions:** J.M.D., C.M.G., T.C.P., M.A.B., and Z.A. all contributed to the data collection. J.M.D., C.M.G., and T.C.P. performed the analysis. J.M.D. wrote the manuscript, with contributions from C.M.G., T.C.P., and Z.A. **Competing interests:** The authors declare that they have no competing interests. **Data and materials availability:** All data needed to evaluate the conclusions in the paper are present in the paper and/or the Supplementary Materials. Additional data related to this paper may be requested from the authors.

Submitted 15 December 2017
Accepted 22 May 2018
Published 4 July 2018
10.1126/sciadv.aar7723

Citation: J. M. DeSilva, C. M. Gill, T. C. Prang, M. A. Bredella, Z. Alemseged, A nearly complete foot from Dikika, Ethiopia and its implications for the ontogeny and function of *Australopithecus afarensis*. *Sci. Adv.* **4**, eaar7723 (2018).

Science Advances

A nearly complete foot from Dikika, Ethiopia and its implications for the ontogeny and function of *Australopithecus afarensis*

Jeremy M. DeSilva, Corey M. Gill, Thomas C. Prang, Miriam A. Bredella and Zeresenay Alemseged

Sci Adv **4** (7), eaar7723.
DOI: 10.1126/sciadv.aar7723